



SORPTION OF VICTORIA BLUE DYE ONTO *MORINDA TINCTORIA* LEAF POWDER AND OPTIMIZATION USING RESPONSE SURFACE METHODOLOGY

Dr.Ch. Asha Immanuel Raju¹, Dr. M. Tukaram Bai², Prof. P. Rajendra Prasad³ and R. Sateesh Kumar⁴

¹Associate Prof, Chemical Engineering Department, Andhra University, Visakhapatnam, AP, India

²Associate Prof, Chemical Engineering Department, Andhra University, Visakhapatnam, AP, India

³Retired Prof, Chemical Engineering Department, Andhra University, Visakhapatnam, AP, India

⁴Research Scholar, Chemical Engineering Department, Andhra University, Visakhapatnam, AP, India

Corresponding Author: Dr. Ch. Asha Immanuel Raju
Email: chairaju@andhrauniversity.edu.in

Abstract

Biosorption of victoria blue dye onto dried *Morinda tinctoria* biomass was contemplated concerning pH, contact time, biosorbent and color focuses. Biosorption is considered to be the most effective method for dye removal in this investigation. Temperature, initial dye concentration, biosorbent dosage, agitation time, and biosorbent size are some of the investigated parameters. The pseudo second order and Lagergren first order models were used in the Kinetic study. Thermodynamics and isotherms like Langmuir, Freundlich, and Temkin were also included in the study. For Optimization and regression analysis, the experimental data were very well fitted and correlated using Response Surface methodology.

Keywords: Biosorption, Dye, Adsorption, RSM, FTIR, SEM.

Introduction

Indian culture is known for its sanskrit, which is considered a part of the world's cultural heritage. As a cultural product with a high added value that must be balanced with superior functionality and quality, sanskrit must be used. Sanskrit texture has antibacterial practical capacity with regular variety greatness expected to acquire buyer interest [1]. There has been a growing interest in the application of various natural dyes to fabrics because the added value of functional textiles with antibacterial capabilities will increase competitive advantage. In the meantime, the textile industry is becoming concerned about the waste generated by the use of additional materials that are harmful to the environment. As a result, antibacterial-capable natural resources from Indonesia require investigation. In India, Noni plants have traditionally been used as a source of dye for cloth for generations. [2].

For typical traditional fabric dyeing, people have used dye from the roots and stem of noni. Roots and stems are frequently utilized as primary dye sources. [3]. Noni's dye ability demonstrated not only a distinct color but also antibacterial and viral activity. [4, 5, 6]. This capability is due to secondary metabolites like anthraquinone, flavonoids, and tannins found in the roots and stems of *Morinda tinctoria* [7]. Since it is a tropical plant, flourishes in India, it guarantees the accessibility and natural manageability. Natural dyes are typically extracted using straightforward methods when used as traditional textile dyes.

A concentrated liquid dye can only be produced using these methods. Be that as it may, there are shortcomings as far as variety soundness and time span of usability of the item thinks. Due to the difficulty of determining the proportion of dye to the fabric to be dyed, product color differences will always occur when concentrates are used in the dyeing process. Additionally, concentrates cannot be stored for an extended period of time due to a problem with power savings. Natural dyes should therefore always be made from scratch. The goals of this study are to produce natural dyes in powder form that are simple to use and can be stored for longer periods of time. Similar to isolated dyes from seed tamarind, the simple method of using saturated saline fluid to extract powder dyes from *Morinda tinctoria* leaves will be tested [8].

In this study, we look into the possibility of using natural dyes from the roots of *Morinda tinctoria* to dye sanskrits. Additionally, the potential economic value of the noni plant derived from sanskrit fabrics and its extensive use in traditional fabric dyeing will be investigated. Thin layer chromatography is used to identify the primary components of extracted dye and the phytochemical composition. Effect of repeated dyeing; UV reflectance spectroscopy will be used to check the color. Infrared spectroscopy is utilized to concentrate on the cooperation among different color cotton textures. In the meantime, the antibacterial measures are being carried out to check the dye's ability to kill bacteria [9]. We anticipate receiving information at the conclusion of this investigation regarding the characteristics of the dye powder made from noni roots, the color that was produced, its interaction with the fabric, and its capacity to fight bacteria. The subsequent process of making traditional sanskrit clothing will use this information.

Experimental Procedure

The current investigation into the biosorption of indigo carmine dye from aqueous solutions onto the biosorbent *hypnea musciformis* powder is carried out both batch-wise and column-wise. The steps of the experimental procedure are as follows:

- ✓ Planning of the biosorbent
- ✓ Portrayal of biosorbent
- ✓ Planning of the stock arrangements
- ✓ Examinations on Harmony Biosorption Interactions

Planning of the biosorbent: *Morinda tinctoria* leaves were gathered from Andhra University hostel premises, Visakhapatnam. The collected biosorbent was then washed several times with water until all of the dirt was gone, then with distilled water. After being sun-dried for fifteen days, the biosorbent was broken up, powdered, and sieved. The obtained powder was used as a biosorbent in this study without any pretreatment.

Portrayal of biosorbent: Biosorbents were characterized by FTIR spectrometry using Spectrum GX of Perkin Elmer. XRD patterns were recorded from 10 to 70⁰ For SEM studies, the dried powders and the corresponding loaded powders were first coated with ultra-thin film of gold by an ion sputter JFC-1100 and then were exposed under a Japanese make electron microscope (JEOL, JXA-8100) for equilibrium studies (agitation time, biosorbent size, pH, dosage, initial concentration & temperature).

Planning of the stock arrangements: By dissolving 1.0 g of 99.9% analytical grade Victoria blue dye in 1000 mL of distilled water, the standard stock solution of Victoria blue dye (1000 mg/L) was created. By diluting the stock solutions with the required amount of deionized water, the dye concentration in the aqueous solution varied from 20 to 200 mg/L. Either 0.1N NaOH or 0.1N HCl was used to adjust the working solution's pH.

Examinations on Harmony Biosorption Interactions: In an orbital shaker, a pre-weighed amount of *Morinda tinctoria* leaves powder was added to a known volume of aqueous solution for a predetermined amount of time to perform the biosorption. The means by which the effects of various parameters were evaluated Using a one-step optimization process, the effects of agitation time, biosorbent size, pH, initial concentration, dosage of biosorbent, and temperature of the aqueous solution on the biosorption of Victoria blue dye were evaluated.

Results and Discussion

The effects of various parameters on biosorption of congo red dye are studied. The measured data consists of initial and final concentration of congo red dye, agitation time, biosorbent size, biosorbent dosage, pH of the aqueous solution and temperature of the aqueous solution. The experimental data are obtained by conducting batch experiments. These are followed by Response Surface Methodology studies involving Central Composite Design and Characterization studies comprising of FTIR and SEM.

Effect of Agitation time

The time it takes for the dye concentration to remain constant during biosorption is known as the duration of equilibrium biosorption. The equilibrium agitation time is depicted in fig. 1. by plotting the percentage of VB dye biosorption against agitation for interaction times ranging from 5 to 180minutes. For the 53m biosorbent dosage of 10gm/L, 24% of the VB dye is biosorbed within the first five minutes. The rate of biosorption rises rapidly up to 25 minutes once it reaches 71%. The constant percentage of biosorption persists after 25minutes under the equilibrium conditions of attainment.

The maximum biosorption of 71% in 50ml of aqueous solution ($C_0=20$ mg/L) is achieved after 25 minutes of agitation with 10 gm/L of biosorbent of 53 m size. Because the biosorbent has a sufficient surface area for the biosorption of VB dye in the early stages, the rate of biosorption is rapid. As the time passes, more VB dye is biosorbed onto the surface of the biosorbent as a result of vanderwall forces of attraction, reducing the available surface area. The biosorbate typically covers the surface in a thin, single-molecule-thick layer. When this monomolecular layer covers the surfaces, the biosorption capacity is exhausted. The maximum 71% of biosorption occurs after 25 minutes. As a result, every other experiment is carried out at this optimal agitation time

[10-11].

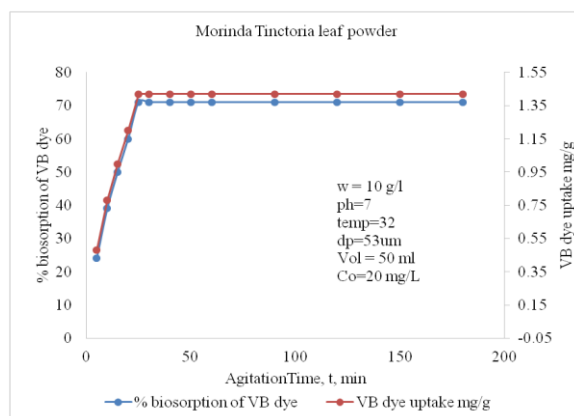


Figure 1: Effect of time on % biosorption of VB dye

Effect of size of biosorbent

Variation in VB dye biosorption percentage with biosorbent size is determined from the aqueous solution. The results are depicted in fig. 2., where the percentage of VB dye that is absorbed by the biosorbent decreases between 53 and 152 micrometers and increases between 71 and 51%. This is to be expected because as the biosorbent's surface area increases, the number of active and freely available sites also increases as the particle size decreases [12-13].

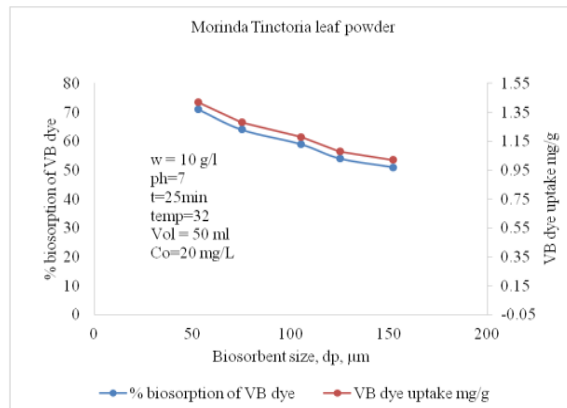


Figure 2: Effect of size on % biosorption of VB dye

Effect of dosage of biosorbent

With an increase in the biosorbent dosage from 10 to 70 g/L, the biosorption of VB dye increased from 81 to 95%, as depicted in fig. 3. This graph compares the percentage of VB dye that is bioabsorbed against the biosorbent dosage for a 53 m biosorbent. Due to the increase in the dosage of the biosorbent, it is evident that there would be more active sites available for VB dye biosorption. The biosorbent of VB dye changes only slightly from 71 to 83.5 percent when dosage is increased from 40 to 70 g/L. As a result, all other experiments are conducted at a dosage of 25 g/L [14-15].

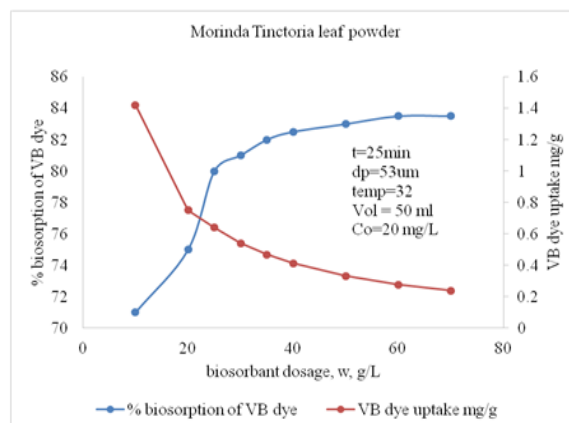


Figure 3: Effect of dosage on % biosorption of VB dye

Effect of initial concentration of the solution, C_0 (mg/L)

Fig. 4. depicts the percentage of VB dye biosorption and its effect on the initial concentration of VB dye in the aqueous solution. In C_0 , the percentage of VB dye that is bioabsorbed rises from 20 to 200 mg/L and decreases from 71 to 49.9 percent. This behavior and the constant number of active sites on the biosorbent are both caused by an increase in the total amount of biosorbate [16-17].

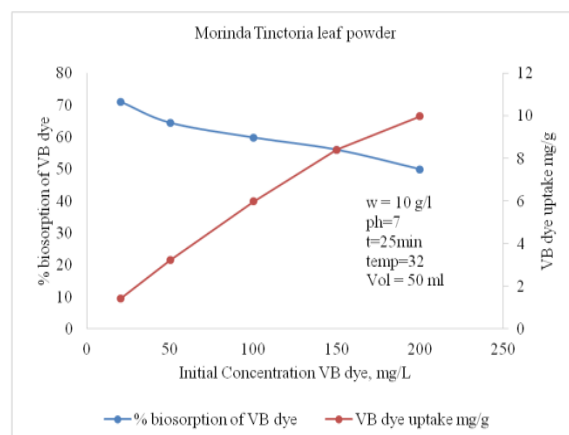


Figure 4: Effect of initial concentration on % biosorption of VB dye

Effect of pH of the solution

By influencing the biosorbent's surface change, pH regulates the degree of ionization and species of the biosorbate. In the current investigation, VB dye biosorption data in the pH range of 2 to 8 are obtained by employing a biosorbent of the aqueous solution with a size of 10 g/L of 53 m. The percentage of VB dye biosorption is shown to be affected by the pH of the aqueous solution in **fig. 5**. After pH 7 it slowly increased, and the margin is very small. Due to competition, the low pH slows biosorption at suitable locations on the biosorbent surface. The VB dye takes the place of the biosorbent-bound H^+ ions, and as the pH rises, this competition becomes less strong [18-19].

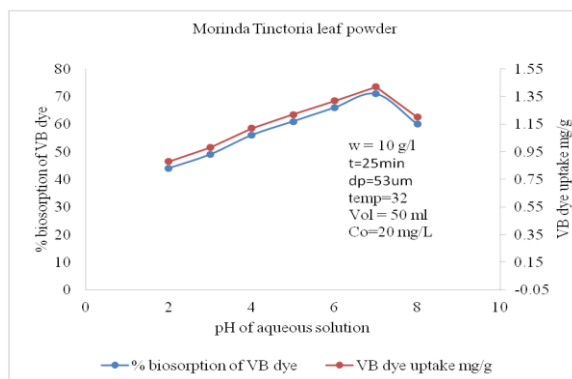


Figure 5: Effect of pH on % biosorption of VB dye

Effect of temperature, T, (K)

Temperature had a significant impact on equilibrium dye uptake in the experiment, which was carried out at temperatures ranging from 283 to 323 K. The effect that changes in temperature have on VB dye uptake is depicted in **fig. 6**. High temperatures encourage dye molecules to diffuse through the internal porous structure of the surface [20-21].

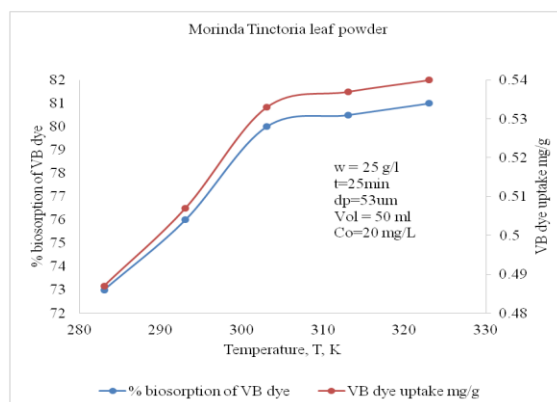


Figure 6: Effect of temperature on % biosorption of VB dye

Isotherms

Langmuir isotherm:

Irving Langmuir developed an isotherm named Langmuir isotherm. It is the most widely used simple two- parameter equation. This simple isotherm is based on following assumptions:

- ✓ Biosorbates are chemically biosorbed at a fixed number of well- defined sites
- ✓ Each site can hold only one biosorbate species
- ✓ All sites are energetically equivalent
- ✓ There is no interaction between the biosorbate species

The Langmuir relationship is hyperbolic and the equation is:

$$q_e/q_m = bC_e / (1+bC_e) \quad \text{----- (a)}$$

Equation can be rearranged as

$$(C_e/q_e) = 1/(bq_m) + C_e/q_m \quad \text{----- (b)}$$

From the plots between (C_e/q_e) and C_e , the slope $\{1/ (bq_m)\}$ and the intercept $(1/b)$ are

calculated. Further analysis of Langmuir equation is made on the basis of separation factor, (R_L) defined as $R_L = 1 / (1 + bC_e)$

$0 < R_L < 1$ indicates favorable adsorption

$R_L > 1$ indicates unfavorable adsorption

$R_L = 1$ indicates linear adsorption

$R_L = 0$ indicates irrepressible adsorption

Langmuir isotherm is drawn for the present data and shown in **Fig. 7**. The equation obtained is: $C_e/q_e = 0.0592C_e + 4.1241$ with a good linearity (correlation coefficient, $R^2 \sim 0.9832$) indicating strong binding of VB dye to the surface of *Morinda tinctoria* leaf powder [22-23].

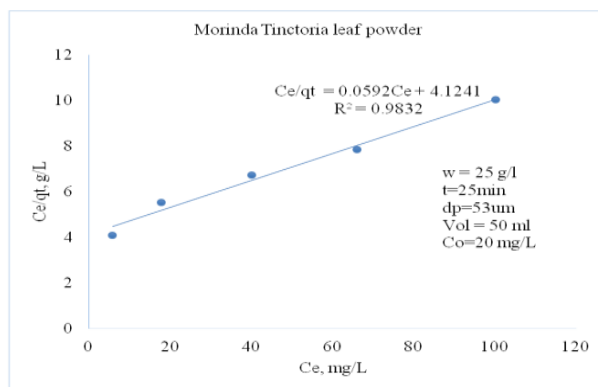


Figure 7: Langmuir isotherm for % biosorption of VB dye

Freundlich isotherm:

Freundlich presented an empirical biosorption isotherm equation that can be applied in case of low and intermediate concentration ranges. It is easier to handle mathematically in more complex calculations.

The Freundlich isotherm is given by

$$q_e = K_f C_e^n \quad \text{----- (c)}$$

Where K_f (mg) represents the biosorption capacity when dye equilibrium concentration and n represent the degree of dependence of biosorption with equilibrium concentration Taking LN on both sides, we get

$$\ln q_e = \ln K_f + n \ln C_e \quad \text{----- (d)}$$

Freundlich isotherm is drawn between $\ln C_e$ and $\ln q_e$ and is shown in **Fig. 8**. for the present data. The resulting equation has a correlation coefficient of 0.9956.

$$\ln q_e = 0.7016 \ln C_e - 0.8562 \quad \text{----- (e)}$$

The 'n' value in the above equation ($n=0.6618$) satisfies the condition of $0 < n < 1$ indicating favorable biosorption [24-25].

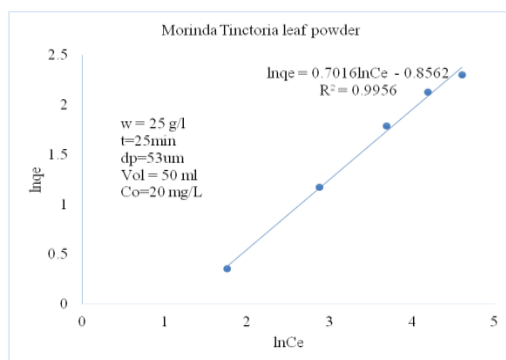


Figure 8: Freundlich isotherm for % biosorption VB dye

Temkin isotherm

Temkin and Pyzhev isotherm equation describes the behavior of many biosorption systems on the heterogeneous surface and it is based on the following equation

$$q_e = RT \ln (A_T C_e) / b_T \text{-----} (f)$$

The linear form of Temkin isotherm can be expressed as

$$q_e = (RT / b_T) \ln (A_T) + (RT / b_T) \ln (C_e) \text{-----} (g)$$

where $A_T = \exp [b(0) \times b(1) / RT]$

$b(1) = RT / b_T$ is the slope

$b(0) = (RT / b_T) \ln (A_T)$ is the intercept and $b = RT / b(1)$

The present data are analysed according to the linear form of Temkin isotherm and the linear plot is shown in **Fig. 9**.

The equation obtained for VB dye biosorption is: $q_e = 3.057 \ln C_e - 4.6725$ with a correlation coefficient 0.9572. The best fit model is determined based on the linear regression correlation coefficient (R). From the **Figs. 7, 8 & 9**, it is found that biosorption data are well represented by Freundlich isotherm with higher correlation coefficient of 0.9956, followed by Temkin and Langmuir isotherms with correlation coefficients of 0.9572 and 0.9832 [26-27] respectively.

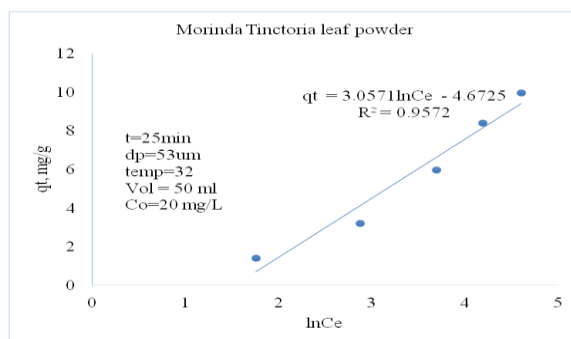


Figure 9: Temkin isotherm for % biosorption of VB dye

Table 1. Isotherm constants (linear method)

Langmuir isotherm	Freundlich isotherm	Temkin isotherm
$q_m = 18.07011 \text{ mg/g}$	$K_f = 0.71184 \text{ mg/g}$	$A_T = 0.33811 \text{ L/mg}$
$K_L = 0.02369$	$n = 0.6618$	$b_T = 738.117$
$R^2 = 0.9832$	$R^2 = 0.9956$	$R^2 = 0.9572$

Kinetics of biosorption

Lagergren First order Kinetics

The request for biosorbate - biosorbent connections have been depicted utilizing motor model. The Lagergren first order model has traditionally been utilized extensively. On account of biosorption went before by dispersion through a limit, the energy generally speaking follows the primary request rate condition of Lagrangen:

$$(dq_t/dt = K_{ad} (q_e - q_t)) \text{ -----(h)}$$

where q_e and q_t are the amounts adsorbed at t , min and equilibrium time and K_{ad} is the rate constant of the pseudo first order biosorption [28-29]

The above equation can be presented as

$$\int (dq_t / (q_e - q_t)) = \int K_{ad} dt \text{ -----(I)}$$

Applying the initial condition $q_t = 0$ at $t = 0$, we get

$$\log (q_e - q_t) = \log q_e - (K_{ad}/2.303) t \text{ -----(j)}$$

In the present study, the kinetics are investigated with 50 mL of aqueous solution ($C_0 = 20 \text{ mg/L}$) at 303 K with the interaction time intervals of 5 min to 180 min. Lagrangen plots of $\log (q_e - q_t)$ versus agitation time (t) for biosorption of VB dye the biosorbent size ($53 \mu\text{m}$) of *Morinda tinctoria* leaf powder in the interaction time intervals of 5 to 180 min are drawn in **fig. 10**.

$$\log (q_e - q_t) = -0.0415 t + 0.205, R^2 = 0.9836 \text{ -----(k)}$$

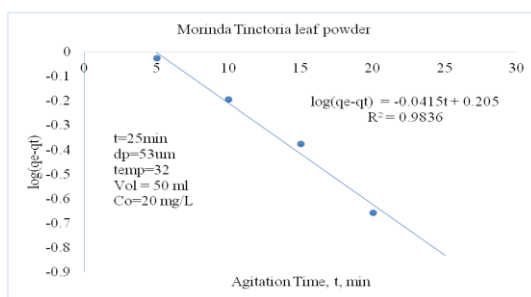


Figure 10: First order kinetics for % biosorption of VB dye

Pseudo Second order Kinetics

Plot of $\log (q_e - q_t)$ versus ' t ' gives a straight line for first order kinetics, facilitating the computation of adsorption rate constant (K_{ad}). If the experimental results do not follow the above equation, they differ in two important aspects:

- $K_{ad} (q_e - q_t)$ does not represent the number of available biosorption sites and
- $\log q_e$ is not equal to the intercept.

In such cases, pseudo second order kinetic equation: $(dq_t/dt) = K (q_e - q_t)^2$ ----- (1)

is applicable, where 'K' is the second order rate constant.

The other form of the above equation is: $(dq_t/(q_e - q_t)^2) = Kdt$ ----- (m)

let $q_e - q_t = x$

$dq_t = dx$

$1/x = Kx + C$ -----(n)

$C = 1/q_e$

at $t = 0$ and $x = q_e$

Substituting these values in above equation, we obtain:

$1/(q_e - q_t) = Kt + (1/q_e)$ ----- (o)

Rearranging the terms, we get the linear form as:

$(t/q_t) = (1/Kq_e^2) + (1/q_e) t$ ----- (p)

The pseudo second order model based on above equation, considers the rate -limiting step as the formation of chemisorptive bond involving sharing or exchange of electrons between the biosorbate and biosorbent. If the pseudo second order kinetics is applicable, the plot of (t/q_t) versus 't' gives a linear relationship that allows computation of q_e and K.

$t/q_t = 0.4186 t + 8.494$, $R^2=0.9937$ ----- (q)

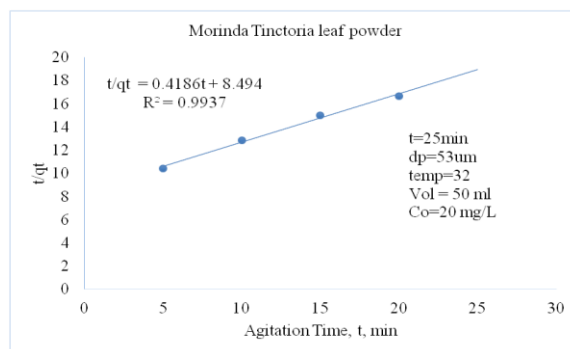


Figure 11: Second order kinetics for % biosorption of VB dye

In the present study, the kinetics are investigated with 50 mL of aqueous solution ($C_0= 20$ mg/L) at 303 K with the interaction time intervals of 5 min to 180 min. Pseudo second order plot of t vs t/q_t for biosorption of VB dye with the biosorbent size (53 μm) of *Morinda tinctoria* leaf powder in the interaction time intervals of 5 to 180 min is drawn in fig. 11. [30-31].

Table 2: Equations and rate constants

Order	Equation	Rate constant	R^2
Lagergren first order	$\log (q_e - q_t) = - 0.0415 t + 0.205$	$0.087514 \text{ min}^{-1}$	0.9836
Pseudo Second order	$t/q_t = 0.4186 t + 8.494$	$0.065219 \text{ g}/(\text{mg}\cdot\text{min})$	0.9937

Thermodynamics of biosorption:

Biosorption is temperature dependant. In general, the temperature dependence is associated with three thermodynamic parameters namely change in enthalpy of biosorption (ΔH), change in entropy of biosorption (ΔS) and change in Gibbs free energy (ΔG).

Enthalpy is the most commonly used thermodynamic function due to its practical significance. The negative value of ΔH will indicate the exothermic/endothermic nature of biosorption and the physical/chemical in nature of sorption. It can be easily reversed by supplying the heat equal to calculated ΔH .

The ΔH is related to ΔG and ΔS as

$$\Delta G = \Delta H - T \Delta S \text{-----(r)}$$

$\Delta S < 1$ indicates that biosorption is impossible whereas $\Delta S > 1$ indicates that the biosorption is possible. $\Delta G < 1$ indicates the feasibility of sorption.

The Vant Hoff's equation is

$$\log (q_e / C_e) = \Delta H / (2.303 RT) + (\Delta S / 2.303 R) \text{-----(s)}$$

$$\log (q_e / C_e) = -155 (1 / T) - 0.425 \text{----- (t)}$$

Where (q_e / C_e) is called the biosorption affinity.

If the value of ΔS is less than zero, it indicates that the process is highly reversible. If ΔS is more than or equal to zero, it indicates the reversibility of process. The negative value for ΔG indicates the spontaneity of biosorption. Whereas the positive value indicates is non spontaneity of sorption.

Experiments are conducted to understand the biosorption behavior varying the temperature from 283 to 323 K. The plot indicating the effect of temperature on biosorption of VB dye for different initial VB dye concentrations is shown in **fig. 12**. The values are $\Delta G = -12012.6$, $\Delta H = 14.5326$ and $\Delta S = 39.6935$ [32-33].

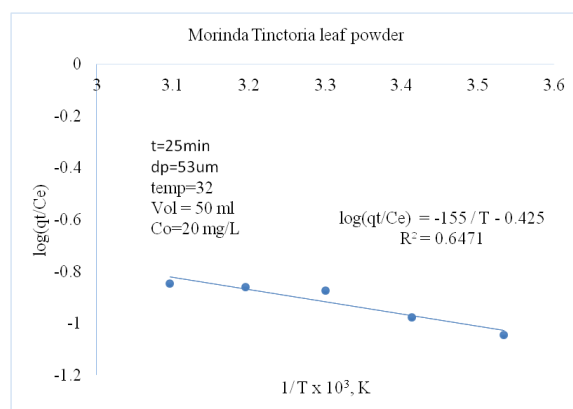


Figure 12: Vantoff's plot for % biosorption of VB dye

Optimization using Response Surface Methodology (RSM):

Optimization of biosorption conditions using CCD

Using Central Composite Design (CCD), the effects of four independent variables on VB dye biosorption—pH, initial VB dye concentration in aqueous solution, dosage of biosorbent, and temperature—are examined. Within the quadratic model, the optimal conditions for the four independent variables pertaining to the degree of VB dye biosorption are established. **Table– 3.** depicts the levels of various process variables for percentage biosorption.

Table 3: Levels of different process variables in coded and un-coded form for % biosorption of VB dye using *Morinda tinctoria* leaf powder

Variable	Name	Range of Levels				
		-2	-1	0	1	2
X1	pH of aqueous solution	5	6	7	8	9
X2	Initial concentration, C _o , mg/L	10	15	20	25	30
X3	Biosorbent dosage, w, g/L	15	20	25	30	35
X4	Temperature, T, K	283	293	303	313	323

Regression equation for the optimization of biosorption is:

% biosorption of VB dye is function of pH of aqueous solution (X1), initial concentration (X2), dosage (X3), and Temperature of aqueous solution (X4). The multiple regression analysis of the experimental data has yielded the following equation:

$$Y = -3394.43 + 86.55X_1 + 8.24X_2 + 7.68X_3 + 19.67X_4 - 5.98 X_1^2 - 0.20 X_2^2 - 0.17 X_3^2 - 0.03 X_4^2 + 0.05X_1X_2 + 0.05X_1X_3 - 0.01X_1X_4 + 0.00X_2X_3 - 0.00X_2X_4 + 0.00X_3X_4 \quad \text{-----} \\ (\text{u})$$

Table- 3. represents the results obtained in CCD. The response obtained in the form of analysis of variance (ANOVA) from regression eq. (10a) is put together in Table– 4. Fischer’s ‘F-statistics’ value is defined as MS_{model}/MS_{error}, where MS is mean square.

Fischer’s ‘F-statistics’ value, having a low probability ‘p’ value, indicates high significance.

Table 4: Results from CCD for VB dye biosorption by *Morinda tinctoria* leaf powder

Run No.	X ₁ , pH	X ₂ , C _o	X ₃ , w	X ₄ , T	% biosorption of VB	
					Experimental	Predicted
1	6	15	20	293	66.78000	66.76000
2	6	15	20	313	68.68000	68.67750
3	6	15	30	293	67.88000	67.90750
4	6	15	30	313	70.12000	70.10000
5	6	25	20	293	64.48000	64.49083
6	6	25	20	313	65.68000	65.71333
7	6	25	30	293	66.12000	66.09333

8	6	25	30	313	67.58000	67.59083
9	8	15	20	293	70.98000	71.00083
10	8	15	20	313	72.58000	72.57333
11	8	15	30	293	73.22000	73.15333
12	8	15	30	313	74.98000	75.00083
13	8	25	20	293	69.82000	69.80667
14	8	25	20	313	70.68000	70.68417
15	8	25	30	293	72.38000	72.41417
16	8	25	30	313	73.58000	73.56667
17	5	20	25	303	58.98000	58.97250
18	9	20	25	303	69.18000	69.18917
19	7	10	25	303	70.18000	70.20250
20	7	30	25	303	66.52000	66.49917
21	7	20	15	303	69.32000	69.30583
22	7	20	35	303	73.32000	73.33583
23	7	20	25	283	73.58000	73.59583
24	7	20	25	323	76.68000	76.66583
25	7	20	25	303	88.00000	88.00000
26	7	20	25	303	88.00000	88.00000
27	7	20	25	303	88.00000	88.00000
28	7	20	25	303	88.00000	88.00000
29	7	20	25	303	88.00000	88.00000
30	7	20	25	303	88.00000	88.00000

Experimental conditions [Coded Values] and observed response values of central composite design with 2⁴ factorial runs, 6- central points and 8- axial points. Agitation time fixed at 40 min and biosorbent size at 53 μm

Table 5: ANOVA of VB dye biosorption for entire quadratic model

Source of variation	SS	Mean square (MS)	F-Value	P> F
Model	1953.534	139.538	162253	0.00000
Error	0.013	0.00086		
Total	1953.547			

Df- degree of freedom; SS- sum of squares; F- factor F; P- probability.
R²=0.99996; R² (adj):0.99992

Table 6: Estimated regression coefficients for the VB dye biosorption onto *Morinda tinctoria* leaf powder

Terms	Regression coefficient	Standard error of the coefficient	t-value	P-value
Mean/Intercept	-3394.43	5.553436	-611.23	0.000000
Dosage, w, g/L (L)	86.55	0.236521	365.94	0.000000
Dosage, w, g/L (Q)	-5.98	0.005512	-1084.87	0.000000
Conc, C ₀ , mg/L (L)	8.24	0.046325	177.82	0.000000
Conc, C ₀ , mg/L (Q)	-0.20	0.000220	-891.20	0.000000
pH (L)	7.68	0.046594	164.86	0.000000
pH (Q)	-0.17	0.000220	-756.50	0.000000
Temperature, T, K (L)	19.67	0.034102	576.77	0.000000
Temperature, T, K (Q)	-0.03	0.000055	-583.69	0.000000
1L by 2L	0.05	0.001443	37.24	0.000000
1L by 3L	0.05	0.001443	34.81	0.000000
1L by 4L	-0.01	0.000722	-11.95	0.000000
2L by 3L	0.00	0.000289	15.76	0.000000
2L by 4L	-0.00	0.000144	-24.08	0.000000
3L by 4L	0.00	0.000144	9.53	0.000000
^a insignificant ($P \geq 0.05$)				

The Fisher's F-test demonstrates that the regression model's ANOVA is sufficient and has a very low probability value ($P_{\text{model}} > F = 0.000000$). Additionally, the fact that the computed F-value is significantly higher than the F-value ($F_{0.05}(14,15) \text{ tabulars} = 2.42$) at the 5% level indicates that the treatment differences are significant enough. The parameter's regression coefficient can be implicated by the Student's t-test, while "p" values can indicate a pattern of interactions among all the factors. It is noted from **Table- 5**. that more huge relating coefficient term can be moved by having high 't' worth and low 'P' esteem. By examining the "t" and "p" values in **Table- 6**, it can be determined that each variable plays a significant role in explaining the individual and interaction effects of independent variables on the biosorption of VB dye in order to anticipate the response. By omitting unrelated terms in eq, the model is reduced to the following form. (v).

$$Y = -3394.43 + 86.55X_1 + 8.24X_2 + 7.68X_3 + 19.67X_4 - 5.98 X_1^2 - 0.20 X_2^2 - 0.17 X_3^2 - 0.03 X_4^2 + 0.05X_1X_2 + 0.05X_1X_3 - 0.01X_1X_4 + 0.00X_2X_3 - 0.00X_2X_4 + 0.00X_3X_4 \quad \text{--- (v)}$$

A positive sign of the coefficient represents an interactive effect i.e., response (% biosorption of VB dye) steps up with increase in effect, whereas a negative sign implies an incompatible effect that means response lowers with an increase in effect.

Measure of the model's variability to the responses indicated is presented by correlation coefficient (R^2). As $R^2 \rightarrow 1$, model is inviolable and the response is estimated better. In our

study, $R^2 = 0.99996$ suggests that 0.004 % of the total variations are not adequately explained by the model. Statistical relevance of the ratio of mean due to regression and mean square due to residual error is tested with the help of ANOVA. F-values implicate that % biosorption can be sufficiently explained by the model equation. If 'P' value is lower than 0.05, the model is considered to be statistically significant at the 95 % confidence level.

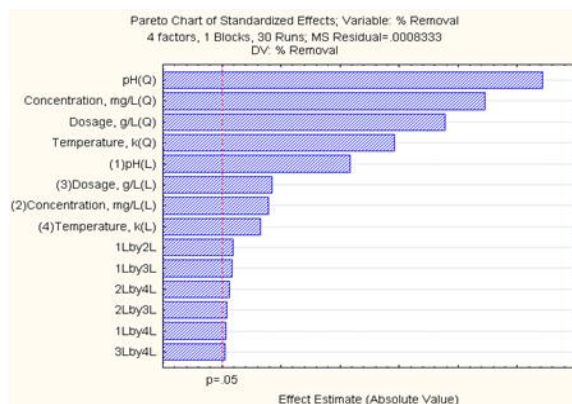


Figure 13: Pareto Chart

The optimal set of conditions for maximum percentage biosorption of VB dye is pH =7.2134, initial VB dye concentration = 19.5547 mg/L, biosorbent dosage = 25.6351 g/L, and temperature = 304.2018 K. The extent of biosorption of VB dye at these optimum conditions was 88.42381 %. It is evident that experimental values of % biosorption are in close agreement with that of predicted by Central Composite Design. Experiments are conducted in triplicate with the above predicted optimal set of conditions and the % biosorption of VB dye is 88 %, which is closer to the predicted % biosorption [34-35].

Interpretation of residual graphs:

The normal probability plot (NPP) is a graphical method for determining whether a data set is more or less normally distributed. The term "residual" refers to the difference between the regression's predicted and observed values. Fig. 14. shows ordinary likelihood plot for the current information. The experimental data are clearly aligned, indicating a normal distribution.

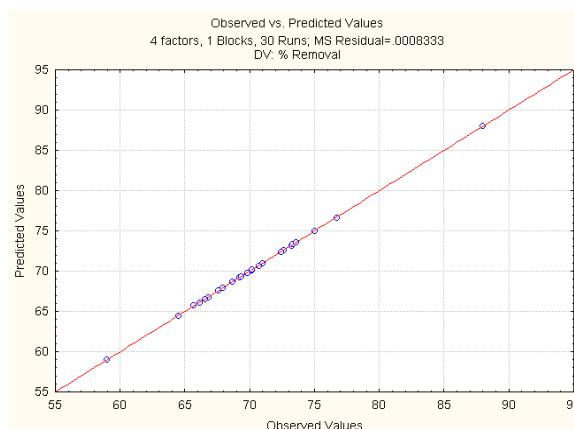


Figure 14: Normal probability plot for % biosorption of VB dye

Interaction effects of biosorption variables

View of response surface contour plots in three dimensions [Fig. 15,16,17,18,19,20] display % biosorption of the VB color utilizing *Morinda tinctoria* leaf powder for various mixes of ward factors. Every one of the plots are depicted as an element of two variables all at once, forcing different elements fixed at zero level. Response surface contour plots demonstrate that the percentage of biosorption is minimal at both low and high levels of the variables. This behavior demonstrates that the input variables are optimal for maximizing the percentage of biosorption. The plots clearly demonstrate how crucial each variable is to the percentage of VB dye biosorption. The anticipated ideal arrangement of conditions for greatest % biosorption of VB dye is:

pH of aqueous solution = 7.2134
 Initial VB dye concentration = 19.5547 mg/L
 Biosorbent dosage = 25.6351 g/L
 Temperature = 304.2018 K
 % biosorption of VB dye = 88.42381

The experimental optimum values are compared with those predicted by CCD in Table- 7. The experimental values are in close agreement with those from CCD.

Table 7: Comparison between optimum values from CCD and experimentation

Variable	CCD	Experimental
pH of aqueous solution	7.2134	7
Initial VB concentration, mg/L	19.5547	20
Biosorbent dosage, w, g/L	25.6351	25
Temperature, K	304.2018	303
% biosorption	88.42381	90

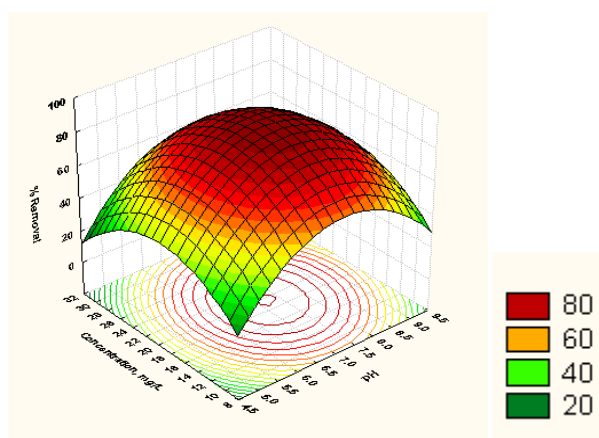


Figure 15: Surface contour plot for the effects of pH and initial concentration of VB dye on % biosorption

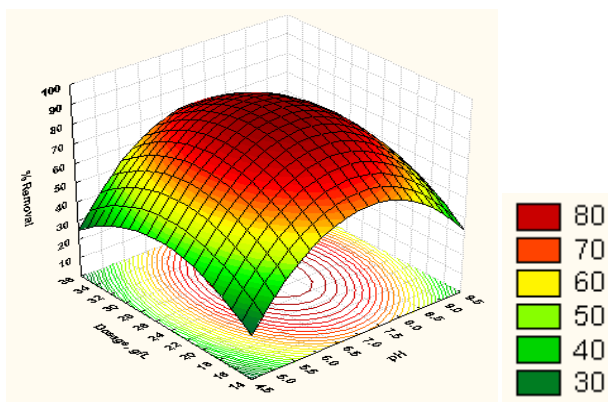


Figure 16: Surface contour plot for the effects of pH and Dosage of VB dye in aqueous solution on % biosorption

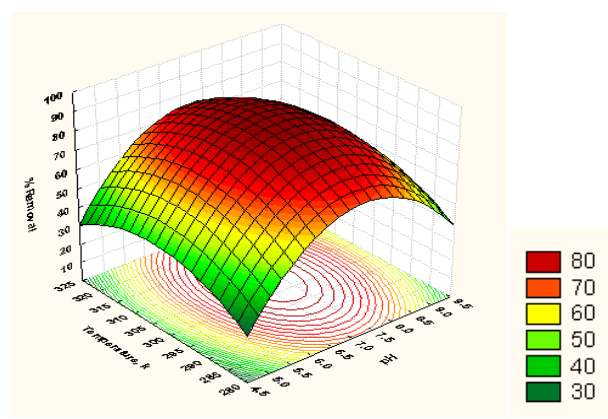


Figure 17: Surface contour plot for the effects of pH and temperature of VB dye in aqueous solution on the % Biosorption

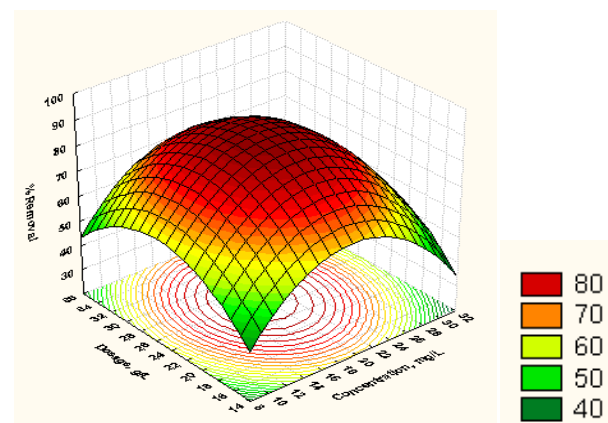


Figure 18: Surface contour plot for the effects of concentration and dosage on % biosorption of VB dye

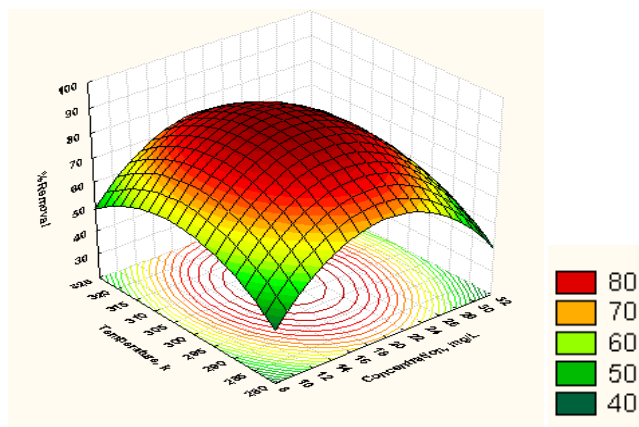


Figure 19: Surface contour plot for the effects of concentration and temperature on % biosorption of VB dye

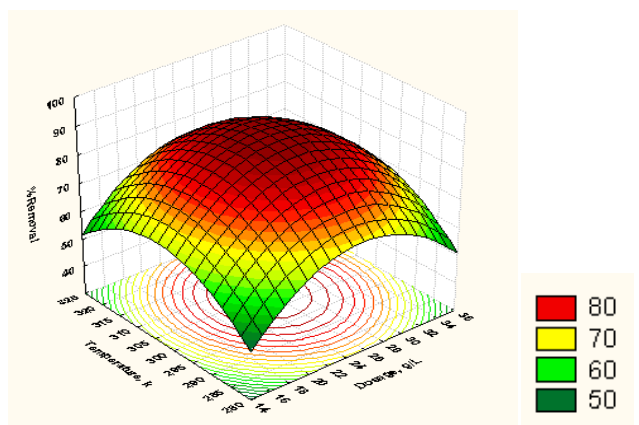


Figure 20: Surface contour plot for the effects of Dosage and temperature on % biosorption of VB dye

FTIR spectrum

FTIR spectrum of untreated *Morinda tinctoria* leaf powder

The FTIR spectrum shown in **fig. 21.** below reveals the presence of Amine C-N stretch at a band width of 1296.02721 cm⁻¹ and the methylene group of lipids at a peak at a band width of 1440.6731 cm⁻¹. At a band width of 1579.53316 cm⁻¹, antisymmetric stretching of RCOOH- is seen. At a band width of 2497.5524 cm⁻¹, amino stretching of N-H is seen. The presence of -OH stretching is confirmed at the peaks of 3479.2159 and 3521.64363 cm⁻¹

FTIR spectrum of treated *Morinda tinctoria* leaf powder

Fig. 22. depicts the treated powder's FTIR spectrum. Amine -C-N stretching is indicated by the peak at 1344.2451 cm⁻¹ wavelength. Additionally, the FTIR spectrum below [21] shows that the Amine N-H stretch mode is present at the wavelengths 2453.19436, 2566.98246, 2725.1286, and 3456.07255 cm⁻¹ [36-37].

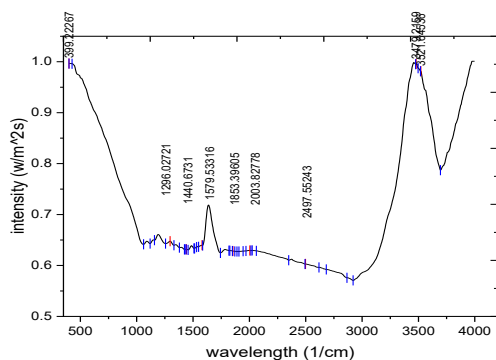


Figure 21: FTIR spectrum of untreated *Morinda tinctoria* leaf powder

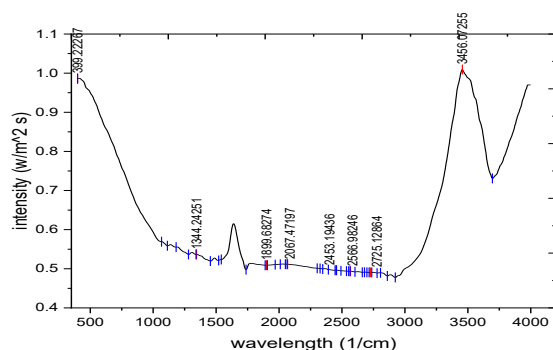


Figure 22: FTIR spectrum of treated *Morinda tinctoria* leaf powder

Table 8: Shift of FTIR peaks for untreated and *Morinda tinctoria* leaf powder treated VB dye

S/N	3A (Peak) cm^{-1}	3C (peak) cm^{-1}	Description
1	399.2267	399.2267	
2	1296.02721	1344.24251	Amine -C-N stretch
3	1440.6731	-	Methylene group of lipids
4	1579.53316	-	Anti-symmetric stretching of carboxylate ion
5	1853.39605	-	
6	-	1899.68274	
7	2003.8277	-	
8	-	2067.4719	
9	2497.55243	2453.19436	Amine N-H stretch mode
10	-	2566.98246	
11	-	2725.12864	
12	-	3456.07255	
13	3521.64536	-	-OH stretch

XRD patterns

X-Ray Diffraction for untreated *Morinda tinctoria* leaf powder

XRD patterns shown in **fig 23 & 24**. for untreated powder do not show very acute or keen and discrete peaks and exhibits minimum amorphous nature. The XRD data shows the peaks at the 2θ values of 45.33, 45.71, 45.86, 45.96, 46.28, 46.51, 46.90, 47.20 corresponds to the C60. 2 S8 (beta, 90 K), 1,2-Bis-crown-5-calix [4] arene, 2C70, 3CS2 solvate, I24 O192 Si96, Na2 O5 Si2, C15 Br3 Cu3 F18 N6, As19 Pb4 S68 Sb21 Tl8 and High-Spin cis Bis(acetonitrile) Tetrakis (triphenylphosphine oxide) iron (II) Triiodide--Acetonitrile (C78 H69 Fe I6 N3 O4 P4). Their d values are 1.999, 1.9832, 1.97712, 1.97305, 1.96015, 1.95099, 1.93867 and 1.92407. The miller indices (h k l) are (-1 0 1), (1 0 1), (1 1 1), (-1 2 1), (1 2 1), (1 11 0), (2 3 0) and (0 7 1) respectively [38-39].

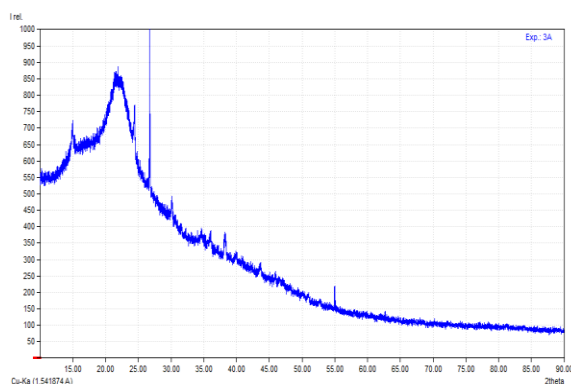


Figure 23: XRD pattern of untreated *Morinda tinctoria* leaf powder

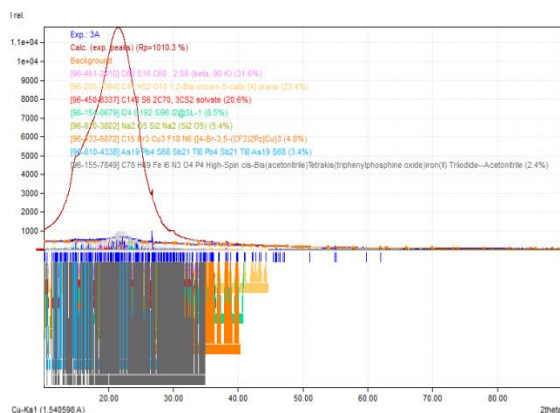


Figure 24: XRD pattern of VB dye untreated *Morinda tinctoria* leaf powder with matching compounds

X-Ray Diffraction for treated *Morinda tinctoria* leaf powder

Fig. 25 & 26. depict XRD patterns of treated VB dye with completely amorphous peaks and extremely sharp peaks. It is clear that biosorption has taken place from the alterations in 2 values and bounds seen both before and after.

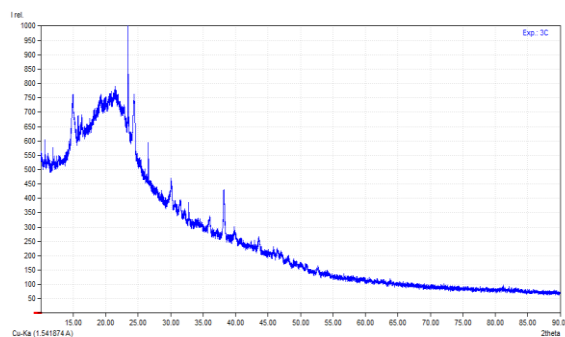


Figure 25: XRD pattern of treated *Morinda tinctoria* leaf powder

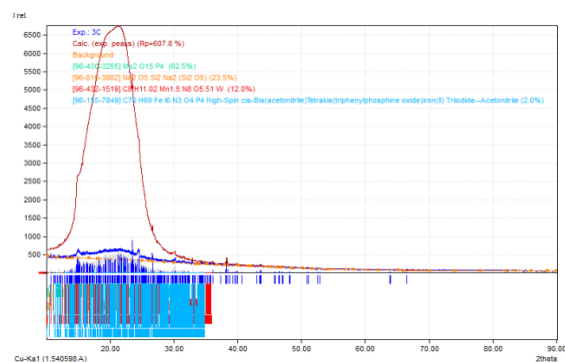


Figure 26: XRD pattern of VB dye treated *Morinda tinctoria* leaf powder with matching compounds

Conclusions

The aim of the study was to determine the suitability of *Jania Rubens* and *Morinda Tinctoria* sorbents for the removal of VB and GV dyes from aqueous solutions. The studies include both periodic and fixed bed studies to assess the potential of these sorbents. The equilibrium, kinetic and thermodynamic studies of VB / GV sorption were carried out experimentally and theoretically. An analysis of the experimental and theoretical data leads to the following conclusions: The equilibrium agitation time for VB dye sorption is 25 minutes. The optimum dosage for sorption is 25 g/L. Maximum extent of sorption is noted at pH = 7. From the predicted values of RSM results, maximum sorption of VB dye (88.42381 %) is observed when the processing parameters are set as pH = 7.2134, w = 25.6351 g/L, Co = 19.5547 mg/L and T = 304.2018 K. The investigation also reveals the endothermic nature of sorption as ΔH is positive (2967.807 J/mole), spontaneity of the sorption as ΔG is negative (-502.1338 J/mole), irreversible nature of sorption as ΔS is positive (8.1375).

References

1. N Stephenson 1993 Art Documentation 107-113
2. B K Majlis 2007 Art Institute of Chicago Museum Studies 33(2) 18-27
3. Sudha D 2016 Textile Society of America's 15th Biennial Symposium Savannah G A
4. Oliveira C, Albuquerque-Junior R, Serafini M, Silva G and Araujo A 2014 MC Proceedings 8(196)

5. Garg P, Tyagi S P, Sinha D J, Singh U P, Malik V and Maccune E R 2014 Saudi Endod. J. 4:122- 7
6. Assi A A, Darwis Y, Abdulbaqi I M, Khan A A, Vuanghao L and Laghari M H 2017 Arab. J. Chem. 10 (5) 691-707
7. Torres M A O, Magalhães, I FB, Mondêgo-Oliveira R, Cortez de Sá J, Rocha AL and Abreu-Silva AL 2017 Phytother. Res.
8. Prabhu K H and Teli M D 2014 J. of Saudi Chem. Soc. 18(6) 864-872
9. Lee A Kim, Y Park, E Hwang, Y Baek, S Cho and H Kim 2017 Textile Res. Journal 0(00)1–1
10. D. R. Paul, W. J. Koros, Effect of partially immobilizing sorption on permeability and the diffusion time lag; Journal of Polymer Science: Polymer Physics Edition; Volume 14, Issue 4; 1976; Pages 675-685.
11. N. J. BARROW, The effect of time on the competition between anions for sorption; European Journal of Soil Science; Volume 43, Issue 3; 1992; Pages 421-428.
12. Minghao Yi, Yuanping Cheng, Zhenyang Wang, Chenghao Wang, Biao Hu, Xinxin He; Effect of particle size and adsorption equilibrium time on pore structure characterization in low pressure N₂ adsorption of coal: An experimental study; Advanced Powder Technology; Volume 31, Issue 10, October 2020, Pages 4275-4281.
13. Juan Wang, Xinhui Liu, Guannan Liu, Zixuan Zhang, Hao Wu, Baoshan Cui, Junhong Bai, Wei Zhang; Size effect of polystyrene microplastics on sorption of phenanthrene and nitrobenzene; Ecotoxicology and Environmental Safety; Volume 173, 30 May 2019, Pages 331-338.
14. Karthikeyan, G., and S. Siva Ilango. "Fluoride sorption using Moringa Indica-based activated carbon." Journal of Environmental Health Science & Engineering 4, no. 1 (2007): 21-28.
15. Sanchez, A. Garcia, E. Alvarez Ayuso, and O. Jimenez De Blas. "Sorption of heavy metals from industrial waste water by low-cost mineral silicates." Clay minerals 34, no. 3 (1999): 469-477.
16. Saadet Yapar, Vesile Özbudak, Ana Dias, Ana Lopes; Effect of adsorbent concentration to the adsorption of phenol on hexadecyl trimethyl ammonium-bentonite; Journal of Hazardous Materials; Volume 121, Issues 1–3, 20 May 2005, Pages 135-139.
17. Singh, Dhanwinder, Ronald G. McLaren, and Keith C. Cameron. "Zinc sorption–desorption by soils: effect of concentration and length of contact period." Geoderma 137, no. 1-2 (2006): 117-125.
18. Q.H.Fan, D.D.Shao, J.Hu, W.S.Wu, X.K.Wang; Comparison of Ni²⁺ sorption to bare and ACT-graft attapulgites: Effect of pH, temperature and foreign ions; Surface Science; Volume 602, Issue 3, 1 February 2008, Pages 778-785.

19. Orhan Altin, Onder H Ozbelge, Timur Dogu, Effect of pH, flow rate and concentration on the sorption of Pb and Cd on montmorillonite: I. Experimental; Journal of Chemical Technology & Biotechnology; 1999.
20. Labuza, T. P., A. Kaanane, and J. Y. Chen. "Effect of temperature on the moisture sorption isotherms and water activity shift of two dehydrated foods." Journal of Food science 50, no. 2 (1985): 385-392.
21. Zhang, Jia-Zhong, and Xiao-Lan Huang. "Effect of temperature and salinity on phosphate sorption on marine sediments." Environmental science & technology 45, no. 16 (2011): 6831-6837.
22. Rajamohan, N. "Equilibrium studies on sorption of an anionic dye onto acid activated water hyacinth roots." African Journal of Environmental Science and Technology 3.11 (2009).
23. Maheria, Kalpana, and Uma Chudasama. "Studies on sorption and elution behaviour of dyes using titanium phosphonate." (2007).
24. Pragathiswaran, C., Abubakkar, B. M., Krishnan, N. A., Govindhan, P., & Usharani, C. ISOTHERM STUDIES ON ADSORPTION OF MALACHITE GREEN ON POWDERED ACTIVATED EUPATORIUM ODORATUM CARBON.
25. Boumediene, M., Benaïssa, H., George, B., Molina, S., & Merlin, A. (2018). Effects of pH and ionic strength on methylene blue removal from synthetic aqueous solutions by sorption onto orange peel and desorption study. J. Mater. Environ. Sci, 9(6), 1700-1711.
26. Lin, C. J., & Lo, S. L. (2005). Effects of iron surface pretreatment on sorption and reduction kinetics of trichloroethylene in a closed batch system. Water Research, 39(6), 1037-1046.
27. Gong, R., Zhong, K., Hu, Y., Chen, J., & Zhu, G. (2008). Thermochemical esterifying citric acid onto lignocellulose for enhancing methylene blue sorption capacity of rice straw. Journal of environmental management, 88(4), 875-880.
28. Gulnaz, O., Kaya, A., Matyar, F., & Arıkan, B. (2004). Sorption of basic dyes from aqueous solution by activated sludge. Journal of hazardous materials, 108(3), 183-188.
29. Özacar, M., & Şengil, İ. A. (2004). Application of kinetic models to the sorption of disperse dyes onto alunite. Colloids and Surfaces A: Physicochemical and engineering aspects, 242(1-3), 105-113.
30. Dizge, N., Aydiner, C., Demirbas, E., Kobya, M., & Kara, S. (2008). Adsorption of reactive dyes from aqueous solutions by fly ash: kinetic and equilibrium studies. Journal of hazardous materials, 150(3), 737-746
31. Aravindhan, R., Rao, J. R., & Nair, B. U. (2007). Removal of basic yellow dye from aqueous solution by sorption on green alga *Caulerpa scalpelliformis*. Journal of hazardous materials, 142(1-2), 68-76.
32. Harley, Stephen J., Elizabeth A. Glascoe, and Robert S. Maxwell. "Thermodynamic study on dynamic water vapor sorption in Sylgard-184." The Journal of Physical Chemistry B 116, no. 48 (2012): 14183-14190.

33. Sullivan, E. J., J. W. Carey, and R. S. Bowman. "Thermodynamics of cationic surfactant sorption onto natural clinoptilolite." *Journal of Colloid and Interface Science* 206, no. 2 (1998): 369-380.
34. Vyavahare, G. D., Gurav, R. G., Jadhav, P. P., Patil, R. R., Aware, C. B., & Jadhav, J. P. (2018). Response surface methodology optimization for sorption of malachite green dye on sugarcane bagasse biochar and evaluating the residual dye for phyto and cytogenotoxicity. *Chemosphere*, 194, 306-315.
35. Sharma, J., Chadha, A. S., Pruthi, V., Anand, P., Bhatia, J., & Kaith, B. S. (2017). Sequestration of dyes from artificially prepared textile effluent using RSM-CCD optimized hybrid backbone based adsorbent-kinetic and equilibrium studies. *Journal of environmental management*, 190, 176-187.
36. Asgher, M., & Bhatti, H. N. (2012). Removal of reactive blue 19 and reactive blue 49 textile dyes by citrus waste biomass from aqueous solution: equilibrium and kinetic study. *The Canadian Journal of Chemical Engineering*, 90(2), 412-419.
37. Papancea, A., Valente, A. J., & Patachia, S. (2010). Diffusion and sorption studies of dyes through PVA cryogel membranes. *Journal of Applied Polymer Science*, 115(3), 1445-1453.
38. Kim, C. Y., Choi, H. M., & Cho, H. T. (1997). Effect of deacetylation on sorption of dyes and chromium on chitin. *Journal of applied polymer science*, 63(6), 725-736.
39. Saiah, F. B. D., Su, B. L., & Bettahar, N. (2009). Nickel–iron layered double hydroxide (LDH): textural properties upon hydrothermal treatments and application on dye sorption. *Journal of Hazardous Materials*, 165(1-3), 206-217.